

Yield-Driven Electromagnetic Optimization via Space Mapping-Based Neuromodels

John W. Bandler,^{1,2} José E. Rayas-Sánchez,² Qi-Jun Zhang³

¹ Simulation Optimization Systems Research Laboratory and the Department of Electrical and Computer Engineering, McMaster University, Hamilton, Ont., Canada L8S 4K1

² Bandler Corporation, P.O. Box 8083, Dundas, Ont., Canada L9H 5E7

³ Department of Electronics, Carleton University, 1125 Colonel By Drive, Ottawa, Canada K1S 5B6

Accepted 3 July 2001

ABSTRACT: Accurate yield optimization and statistical analysis of microwave components are crucial ingredients for manufacturability-driven designs in a time-to-market development environment. Yield optimization requires intensive simulations to cover the entire statistic of possible outcomes of a given manufacturing process. Performing direct yield optimization using accurate full-wave electromagnetic simulations does not appear feasible. In this article, an efficient procedure to realize electromagnetics (EM) based yield optimization and statistical analysis of microwave structures using space mapping-based neuromodels is proposed. Our technique is illustrated by the EM-based statistical analysis and yield optimization of a high temperature superconducting (HTS) microstrip filter. © 2002 John Wiley & Sons, Inc. Int J RF and Microwave CAE 12: 79–89, 2002.

Keywords: neural network applications; space mapping; optimization methods; design automation; EM optimization; neural space mapping; statistical analysis; yield optimization; design centering; microwave circuits; microstrip filters; neural modeling

I. INTRODUCTION

Electromagnetic (EM) full-wave field solvers are regarded as highly accurate to predict the behavior of microwave structures. With the increasing availability of commercial EM simulators, it is very desirable to include them in the statistical

analysis and yield-driven design of microwave circuits. Given the high cost in computational effort imposed by the EM simulators, creative procedures must be researched to efficiently use them for statistical analysis and design.

Yield-driven EM optimization was proposed in [1] by using multidimensional quadratic models that approximate the EM model responses for efficient and accurate evaluations. A more integrated CAD environment for statistical analysis and yield-driven circuit design was later proposed in [2], where the quadratic modeling techniques and interpolation techniques (to deal with the discretization of the geometrical parameters of the EM structure) were unified.

For the first time, we propose in this article the use of space mapping (SM)-based neuromodels for efficient and accurate EM-based

Correspondence to: John W. Bandler; e-mail: bandler@mcmaster.ca

Contract grant sponsor: Natural Sciences and Engineering Research Council of Canada.

Contract grant number: OGP0007239.

Contract grant number: STR234854-00.

Contract grant sponsor: Micronet Network of Centres of Excellence and Bandler Corporation.

Contract grant sponsor: Instituto Tecnológico y de Estudios Superiores de Occidente, Mexico.

statistical analysis and yield optimization of microwave structures. We briefly review the use of artificial neural networks (ANNs) for the design by optimization of microwave circuits. We mathematically formulate the yield optimization problem using SM-based neuromodels. A general equation to express the relationship between the fine and coarse model sensitivities through a nonlinear, frequency-sensitive neuromapping is presented. We illustrate our technique by the yield analysis and optimization of a high-temperature superconducting (HTS) quarter-wave parallel coupled-line microstrip filter.

II. A BRIEF REVIEW ON OPTIMIZATION OF MICROWAVE CIRCUITS USING NEURAL NETWORKS

Neural networks have been extensively used for modeling in many different variations [3–5]. In contrast, the use of neural networks for design by optimization is at an earlier stage; a few variations in the use of neural networks for optimization of microwave circuits have been reported.

The most widely used technique for neural optimization of microwave circuits consists of generating a neuromodel of the microwave circuit within a certain training region of the design parameters, and then applying conventional optimization to the neuromodel to find the optimal solution that yields the desired response. A neuromodel can be developed for the whole microwave circuit to be optimized, or in a decomposed fashion, where small neuromodels are developed for each individual component in the circuit, which are later connected by circuit theory. Full-wave EM simulations are typically employed to generate the training data. The generalization ability of the neuromodel(s) is controlled during the training process by using validation data and testing data, also obtained from EM simulations. Examples of this neural optimization approach can be found in [6–10].

The previous neural optimization approach has two main disadvantages: the time required to generate sufficient training, validation and testing samples, and the unreliability of the optimal solution when it lies outside the training region, due to the poor extrapolation performance of ANNs.

One way to decrease the amount of up-front EM simulations is proposed in [3], where the neuromodel to be optimized consists of several neural

networks, each of them specialized for a cluster of responses that were previously identified.

Both limitations of the conventional neural optimization approach have been alleviated by incorporating prior knowledge into the neural network structure, following an EM-ANN approach [11], or a neural space mapping (NSM) approach [4]. In [12], an EM-ANN approach was used to optimize a CPW patch antenna. Similarly, an end-coupled bandpass filter in a 2-layer configuration was designed in [13] following also an EM-ANN approach. NSM optimization was used in [14, 15] to design a bandstop microstrip filter with open stubs and an HTS microstrip filter; NSM optimization has the additional advantage of not requiring either validation or training data, because it employs a neural network growing strategy to control the generalization performance.

A fifth variation for the design of microwave circuits with ANNs is by using synthesis neural networks. A synthesis neural network is trained to learn the mapping from the responses to the design parameters of the microwave circuit. In this sense, a conventional neuromodel becomes an analysis neural network. The problem of training a synthesis neural network is known as the inverse modeling problem, because the input and output variables are interchanged.

The analysis problem is characterized by a single-value mapping: given a vector of design parameters we have only one possible vector of responses. However, for inverse problems, the mapping can often be multivalued: a given vector of responses can be generated by several different vectors of design parameters. This leads the synthesis neural network to make poor generalizations. Another complication of the inverse modeling problem is the coverage of the input space by the training data, because the full characterization of the input space (microwave circuit responses) is usually not available.

A dedicated algorithm for the design of multi-layer asymmetric coupled transmission structures using a combination of analysis and synthesis neural networks was successfully developed in [16]. Here, the input space of the synthesis neural network is not the set of S parameters, but a set of LC parameters that are later translated into the conventional responses.

In practice, random variations in the manufacturing process of a microwave device may result in a significant percentage of the produced devices not meeting the specifications. When designing, it

is essential to account for these inevitable uncertainties. Many significant contributions have been made to the statistical analysis and design of microwave circuits (e.g., [1, 2, 17]). Nevertheless, the use of neuromodels for statistical analysis and yield optimization of microwave circuits has not been extensively exploited [18].

We propose in this article the use of SM-based neuromodels for efficient EM-based statistical analysis and yield optimization of microwave circuits.

III. STATISTICAL CIRCUIT ANALYSIS AND DESIGN: PROBLEM FORMULATION

Let $\mathbf{x} \in \mathfrak{R}^n$ represent the vector of n design parameters of the microwave device, whose r responses at frequency ω are contained in vector $\mathbf{R}(\mathbf{x}, \omega) \in \mathfrak{R}^r$ (for example, $\mathbf{R}(\mathbf{x}, \omega)$ might contain the real and imaginary parts of S_{11} at 10 GHz for a given physical structure).

The design goals are defined by a vector $\mathbf{S}_u(\omega) \in \mathfrak{R}^r$ of upper specifications and a vector $\mathbf{S}_l(\omega) \in \mathfrak{R}^r$ of lower specifications imposed on the responses $\mathbf{R}(\mathbf{x}, \omega)$ at each frequency of interest. A lower specification on the k th response at frequency ω requires $\mathbf{R}_k(\mathbf{x}, \omega) \geq \mathbf{S}_{lk}(\omega)$ whereas an upper specification requires $\mathbf{R}_k(\mathbf{x}, \omega) \leq \mathbf{S}_{uk}(\omega)$. It is possible to impose both a lower and an upper specification on a single response.

Two error vectors $\mathbf{e}_u, \mathbf{e}_l \in \mathfrak{R}^r$ can be used to measure the degree to which a response satisfies or violates the specifications,

$$\mathbf{e}_l(\mathbf{x}, \omega) = \mathbf{S}_l(\omega) - \mathbf{R}(\mathbf{x}, \omega), \quad (1)$$

$$\mathbf{e}_u(\mathbf{x}, \omega) = \mathbf{R}(\mathbf{x}, \omega) - \mathbf{S}_u(\omega). \quad (2)$$

Nonnegative weighting factors can be included in (1) and (2) for scaling purposes. In practice, vectors (1) and (2) are sampled at a finite set of frequency points of interest, not necessarily overlapping. The corresponding two sets of vectors can be combined in a single error vector

$$\mathbf{e}(\mathbf{x}) = [\mathbf{e}_{l1}^T \quad \mathbf{e}_{l2}^T \cdots \mathbf{e}_{u1}^T \quad \mathbf{e}_{u2}^T \cdots]^T, \quad (3)$$

whose dimensionality is denoted by M . Clearly, negative components in \mathbf{e} indicate satisfaction of the corresponding specifications.

In the nominal design, we are interested in finding a single vector of design parameters \mathbf{x}^* , called

optimal nominal solution, for which the responses $\mathbf{R}(\mathbf{x}^*)$ optimally satisfy the design specifications \mathbf{S}_u and \mathbf{S}_l at all frequency points of interest. Following [19], this task can be formulated as a minimax optimization problem

$$\mathbf{x}^* = \arg \min_{\mathbf{x}} U(\mathbf{x}) \quad (4)$$

$$U(\mathbf{x}) = \max_j \mathbf{e}_j(\mathbf{x}), \quad (5)$$

where $\mathbf{e}_j(\mathbf{x})$ is the j th element in the error vector (3), with $j = 1, \dots, M$.

In the statistical approach to circuit design, we take into account that the design parameters of the manufactured device outcomes \mathbf{x}^k are actually spread around the nominal point \mathbf{x} according to their statistical distributions and tolerances. These parameters can be represented as

$$\mathbf{x}^k = \mathbf{x} + \Delta \mathbf{x}^k, \quad k = 1, 2, \dots, N, \quad (6)$$

where N is the number of such outcomes. We associate with each outcome an acceptance index defined by

$$I_a(\mathbf{x}^k) = \begin{cases} 1, & \text{if } U(\mathbf{x}^k) \leq 0, \\ 0, & \text{if } U(\mathbf{x}^k) > 0. \end{cases} \quad (7)$$

If N is sufficiently large for statistical significance, we can approximate the yield Y at the nominal point \mathbf{x} by using

$$Y(\mathbf{x}) \approx \frac{1}{N} \sum_{k=1}^N I_a(\mathbf{x}^k). \quad (8)$$

An error vector $\mathbf{e}(\mathbf{x}^k) \in \mathfrak{R}^M$ is associated with each circuit outcome \mathbf{x}^k according to (1)–(3). Following [19], the optimal yield solution \mathbf{x}^{Y^*} can be found by solving

$$\mathbf{x}^{Y^*} = \arg \min_{\mathbf{x}} \sum_{k \in K} \alpha_k H_1(\mathbf{x}^k), \quad (9)$$

$$K = \{k | H_1(\mathbf{x}^k) > 0\}, \quad (10)$$

where $H_1(\mathbf{x}^k)$ is the generalized l_1 function

$$H_1(\mathbf{x}^k) = \begin{cases} \sum_{j \in J} \mathbf{e}_j(\mathbf{x}^k) & \text{if } J(\mathbf{x}^k) \text{ is} \\ & \text{not empty,} \\ [\sum_{j=1}^M [\mathbf{e}_j(\mathbf{x}^k)]^{-1}]^{-1} & \text{if } J(\mathbf{x}^k) \text{ is} \\ & \text{empty,} \end{cases} \quad (11)$$

$$J = \{j | \mathbf{e}_j(\mathbf{x}^k) \geq 0\} \quad (12)$$

and α_k are positive multipliers calculated from

$$\alpha_k = \frac{1}{|H_1(\mathbf{x}^{(0)} + \Delta \mathbf{x}^k)|}, \quad k = 1, 2, \dots, N, \quad (13)$$

where $\mathbf{x}^{(0)}$ is the starting point, for which a good candidate is the optimal nominal solution \mathbf{x}^* . It is seen that the optimal yield objective function in (9) equals the number of failed circuits N_{fail} at the starting point and provides a continuous approximation to N_{fail} during optimization. If necessary, yield optimization can be restarted with α_k updated with the current solution. We use in this article the highly efficient implementation of yield analysis and optimization available in OSA90/hopeTM [20].

IV. YIELD ANALYSIS AND OPTIMIZATION USING SM-BASED NEUROMODELS

We propose the use of SM-based neuromodels to perform accurate and efficient yield analysis and optimization of microwave devices. The aim is to combine the computational efficiency of coarse models (typically equivalent circuit models) with the accuracy of fine models (typically EM simulators). We assume that the SM-based neuromodel is already available, obtained either from a modeling process [4] or from an optimization process [15].

Let the vectors $\mathbf{x}_c, \mathbf{x}_f \in \mathfrak{R}^n$ represent the design parameters of the coarse and fine models, respectively. In general, the operating frequency ω , used by the fine model, can be different to that used by the coarse model, denoted as ω_c . Let $\mathbf{R}_c(\mathbf{x}_c, \omega_c), \mathbf{R}_f(\mathbf{x}_f, \omega) \in \mathfrak{R}^r$ represent the coarse and fine model responses at the frequencies ω_c and ω , respectively. We denote the corresponding SM-based neuromodel responses at frequency ω as $\mathbf{R}_{\text{SMBN}}(\mathbf{x}_f, \omega)$, given by

$$\mathbf{R}_{\text{SMBN}}(\mathbf{x}_f, \omega) = \mathbf{R}_c(\mathbf{x}_c, \omega_c) \quad (14)$$

with

$$\begin{bmatrix} \mathbf{x}_c \\ \omega_c \end{bmatrix} = \mathbf{P}(\mathbf{x}_f, \omega), \quad (15)$$

where the mapping function \mathbf{P} is implemented by a neural network following any of the five neuromapping variations (SM, FDSM, FSM, FM or FPSM) described in [15]. As stated before, we assume that a suitable mapping function \mathbf{P} has

already been found (i.e., a neural network with suitable complexity has already been trained).

If the SM-based neuromodel is properly developed,

$$\mathbf{R}_f(\mathbf{x}_f, \omega) \approx \mathbf{R}_{\text{SMBN}}(\mathbf{x}_f, \omega) \quad (16)$$

for all \mathbf{x}_f and ω in the training region. The Jacobian of the fine model responses w.r.t. the fine model parameters, $\mathbf{J}_f \in \mathfrak{R}^{r \times n}$, is defined as

$$\mathbf{J}_f = \begin{bmatrix} \frac{\partial R_f^1}{\partial x_{f1}} & \cdots & \frac{\partial R_f^1}{\partial x_{fn}} \\ \vdots & \ddots & \vdots \\ \frac{\partial R_f^r}{\partial x_{f1}} & \cdots & \frac{\partial R_f^r}{\partial x_{fn}} \end{bmatrix}. \quad (17)$$

On the other hand, the Jacobian of the coarse model responses w.r.t. the coarse model parameters and mapped frequency, denoted by $\mathbf{J}_c \in \mathfrak{R}^{r \times (n+1)}$, is given by

$$\mathbf{J}_c = \begin{bmatrix} \frac{\partial R_c^1}{\partial x_{c1}} & \cdots & \frac{\partial R_c^1}{\partial x_{cn}} & \frac{\partial R_c^1}{\partial \omega_c} \\ \vdots & \ddots & \vdots & \vdots \\ \frac{\partial R_c^r}{\partial x_{c1}} & \cdots & \frac{\partial R_c^r}{\partial x_{cn}} & \frac{\partial R_c^r}{\partial \omega_c} \end{bmatrix}, \quad (18)$$

while the Jacobian of the mapping w.r.t. the fine model parameters, denoted by $\mathbf{J}_p \in \mathfrak{R}^{(n+1) \times n}$, is given by

$$\mathbf{J}_p = \begin{bmatrix} \frac{\partial x_{c1}}{\partial x_{f1}} & \cdots & \frac{\partial x_{c1}}{\partial x_{fn}} \\ \vdots & \ddots & \vdots \\ \frac{\partial x_{cn}}{\partial x_{f1}} & \cdots & \frac{\partial x_{cn}}{\partial x_{fn}} \\ \frac{\partial \omega_c}{\partial x_{f1}} & \cdots & \frac{\partial \omega_c}{\partial x_{fn}} \end{bmatrix}. \quad (19)$$

From (17)–(19), the sensitivities of the fine model responses can be approximated using

$$\mathbf{J}_f \approx \mathbf{J}_c \mathbf{J}_p. \quad (20)$$

The accuracy of the approximation of \mathbf{J}_f using (20) will depend on how well the SM-based neuromodel reproduces the behavior of the fine model in the training region, i.e., it will depend on the accuracy of the approximation (16).

Equation (20) represents a generalization of the lemma found in [21], where a linear, frequency-insensitive mapping function was assumed. Naturally, (20) will be accurate over a larger region because the mapping is nonlinear and frequency-sensitive, which has proved to be a very significant advantage when dealing with coarse models based on quasistatic approximations.

If the mapping is implemented with a 3-layer perceptron with h hidden neurons, then (15) is

given by

$$\mathbf{P}(\mathbf{x}_f, \omega) = \mathbf{W}^o \Phi(\mathbf{x}_f, \omega) + \mathbf{b}^o, \quad (21)$$

$$\Phi(\mathbf{x}_f, \omega) = [\varphi(s_1) \varphi(s_2) \cdots \varphi(s_h)]^T, \quad (22)$$

$$\mathbf{s} = \mathbf{W}^h \begin{bmatrix} \mathbf{x}_f \\ \omega \end{bmatrix} + \mathbf{b}^h, \quad (23)$$

where $\mathbf{W}^o \in \mathfrak{N}^{(n+1) \times h}$ is the matrix of output weighting factors, $\mathbf{b}^o \in \mathfrak{N}^{(n+1)}$ is the vector of output bias elements, $\Phi \in \mathfrak{N}^h$ is the vector of hidden signals, $\mathbf{s} \in \mathfrak{N}^h$ is the vector of activation potentials, $\mathbf{W}^h \in \mathfrak{N}^{h \times (n+1)}$ is the matrix of hidden weighting factors, $\mathbf{b}^h \in \mathfrak{N}^h$ is the vector of hidden bias elements and h is the number of hidden neurons. A typical choice for the nonlinear activation functions is hyperbolic tangents, i.e., $\varphi(\cdot) = \tanh(\cdot)$. All the internal parameters of the neural network, \mathbf{b}^o , \mathbf{b}^h , \mathbf{W}^o and \mathbf{W}^h are constant because the SM-based neuromodel has been already developed.

The Jacobian \mathbf{J}_p is obtained from (21)–(23) as

$$\mathbf{J}_p = \mathbf{W}^o \mathbf{J}_\Phi \mathbf{W}^h, \quad (24)$$

where $\mathbf{J}_\Phi \in \mathfrak{N}^{h \times h}$ is a diagonal matrix given by $\mathbf{J}_\Phi = \text{diag}(\varphi'(s_j))$, with $j = 1, \dots, h$.

If the SM-based neuromodel uses a 2-layer perceptron, then the Jacobian \mathbf{J}_p is simply

$$\mathbf{J}_p = \mathbf{W}^o \quad (25)$$

which corresponds to the case of a frequency-sensitive linear mapping. Notice that by substituting (25) in (20) and assuming a frequency-insensitive neuromapping we obtain the lemma found in [21], because in the case of a 2-layer perceptron with no frequency dependence, $\mathbf{W}^o \in \mathfrak{N}^{n \times n}$.

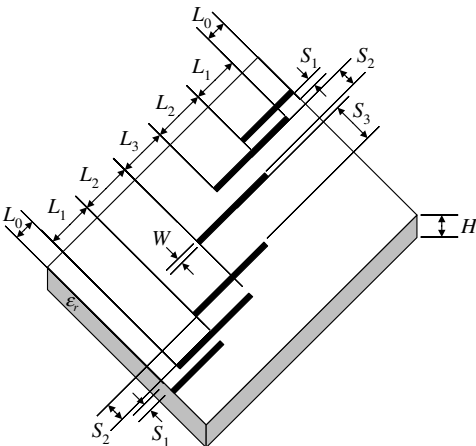


Figure 1. HTS quarter-wave parallel coupled-line microstrip filter.

V. EXAMPLE

Consider an HTS quarter-wave parallel coupled-line microstrip filter [4, 15]. The physical structure of the HTS filter is illustrated in Figure 1.

L_1 , L_2 , and L_3 are the lengths of the parallel coupled-line sections and S_1 , S_2 , and S_3 are the gaps between the sections. The width W is the same for all the sections as well as for the input and output lines of length L_0 . A lanthanum aluminate substrate with thickness H and dielectric constant ε_r is used.

The specifications are $|S_{21}| \geq 0.95$ in the passband and $|S_{21}| \leq 0.05$ in the stopband, where the stopband includes frequencies below 3.967 GHz and above 4.099 GHz, and the passband lies in the range [4.008–4.058 GHz].

OSA90/hopeTM [20] built-in linear elements microstrip line (MSL), two-conductor symmetrical coupled microstrip lines (MSCL) and open circuit (OPEN) connected by circuit theory over the same microstrip substrate definition (MSUB) are taken as the “coarse” model, whose schematic representation is illustrated in Figure 2.

Sonnet’s *em*TM [22] driven by EmpipeTM [20] was employed as the fine model, using a high-resolution grid with a 1 mil × 1 mil cell size.

A. Yield Analysis and Optimization Assuming Symmetry

The SM-based neuromodel of the HTS filter obtained in [4] is used to perform yield analysis and optimization. This model was obtained assuming that the design parameters are $\mathbf{x}_f = [L_1 L_2 L_3 S_1 S_2 S_3]^T$, and taking $L_0 = 50$ mil, $H = 20$ mil, $W = 7$ mil, $\varepsilon_r = 23.425$, loss tangent $= 3 \times 10^{-5}$; the metalization was considered lossless. The corresponding SM-based neuromodel is illustrated in Figure 3, which implements a frequency partial-space-mapped neuromapping with 7 hidden neurons, mapping only L_1 , S_1 and the frequency (3LP:7-7-3). L_{1c} and S_{1c} in Figure 3 denote the corresponding two physical dimensions

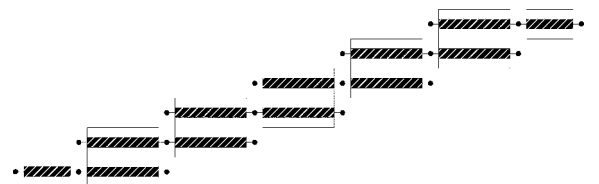


Figure 2. Schematic representation of the coarse model for the HTS filter.

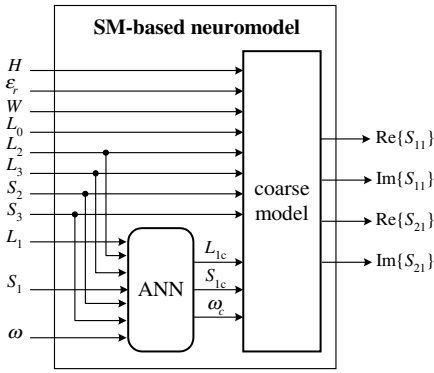


Figure 3. SM-based neuromodel of the HTS filter for yield analysis assuming symmetry (L_{1c} and S_{1c} correspond to L_1 and S_1 as used by the coarse model).

as used by the coarse model, i.e., after being transformed by the mapping. Notice from Figure 1 that it is assumed that the structure of the HTS filter poses vertical and horizontal physical symmetry.

Applying direct minimax optimization to the coarse model, we obtain the optimal coarse solution $\mathbf{x}_c^* = [188.33 \ 197.98 \ 188.58 \ 21.97 \ 99.12 \ 111.67]^T$ (mil). The coarse model response at \mathbf{x}_c^* is shown in Figure 4. The fine model response at the optimal coarse solution is shown in Figure 5 using a fine frequency sweep.

We apply direct minimax optimization to the SM-based neuromodel, taking \mathbf{x}_c^* as the starting point, to obtain the optimal SM-based neuromodel nominal solution $\mathbf{x}_{\text{SMBN}}^* = [185.79 \ 194.23 \ 184.91 \ 21.05 \ 82.31 \ 89.32]^T$ (mil). Figure 6 shows excellent agreement between the SM-based neuromodel response and the fine model response at $\mathbf{x}_{\text{SMBN}}^*$.

To realize yield analysis, we consider 0.2% of variation for the dielectric constant and for the loss tangent, as well as 75 micron of variation for the physical dimensions, as suggested in [23], with

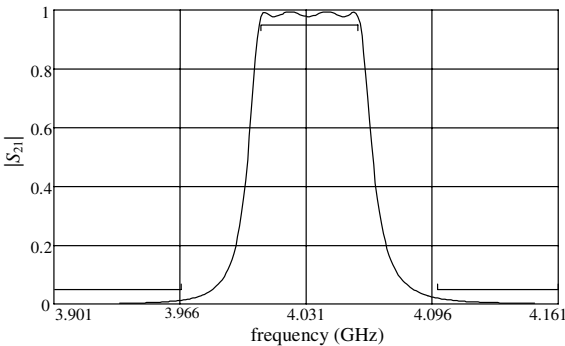


Figure 4. Optimal coarse model response.

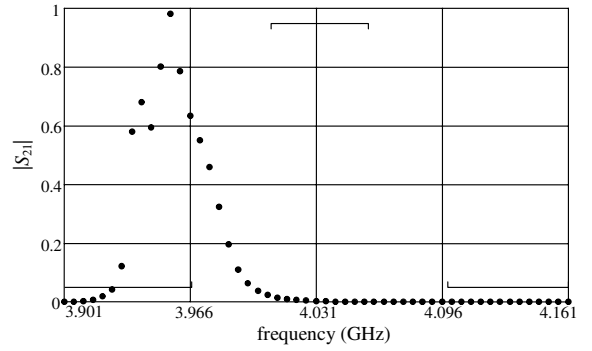


Figure 5. Fine model response at optimal coarse solution.

uniform statistical distributions. These tolerances are larger than other typical manufacturing tolerances reported in the literature [3].

We perform Monte Carlo yield analysis of the SM-based neuromodel around $\mathbf{x}_{\text{SMBN}}^*$ with 500 outcomes using OSA90/hopeTM [20]. The responses for 50 of those outcomes are shown in Figure 7. The yield calculation is shown in Figure 8. A yield of only 18.4% is obtained at $\mathbf{x}_{\text{SMBN}}^*$, which is reasonable considering the well-known high sensitivity of this microstrip circuit.

Performing yield analysis using 500 outcomes with the SM-based neuromodel of the HTS filter takes a few tens of seconds on a conventional computer (PC AMD 640 MHz, 256 M RAM, on Windows NT 4.0), whereas a single outcome calculation for the same circuit using an EM simulation takes around 5 hours on the same computer. The SM-based neuromodel makes feasible the EM-based yield analysis of this complex microwave structure.

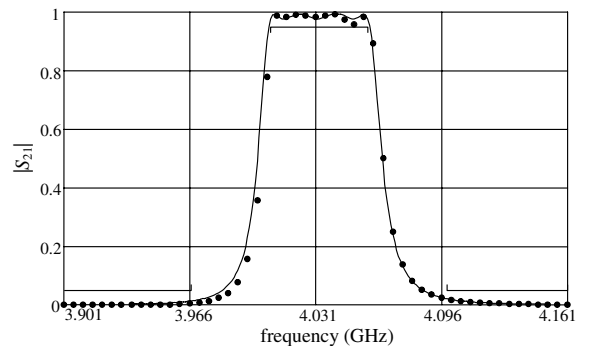


Figure 6. Fine model response and SM-based neuromodel response at the optimal nominal solution $\mathbf{x}_{\text{SMBN}}^*$.

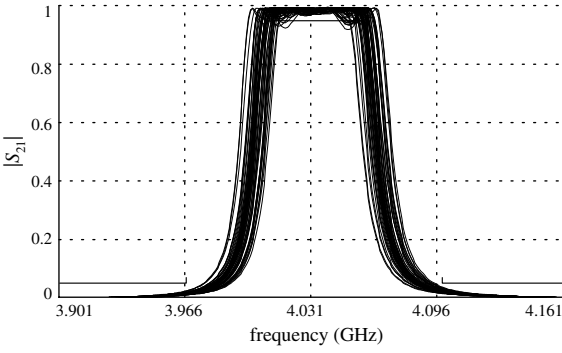


Figure 7. Monte Carlo yield analysis of the SM-based neuromodel responses around the optimal nominal solution $\mathbf{x}_{\text{SMBN}}^*$ with 50 outcomes.

We then apply yield optimization to the SM-based neuromodel with 500 outcomes using the Yield-Huber optimizer available in OSA90/hopeTM [20], obtaining the following optimal yield solution: $\mathbf{x}_{\text{SMBN}}^{Y*} = [183.04 \ 196.91 \ 182.22 \ 20.04 \ 77.67 \ 83.09]^T$ (mil). The corresponding responses for 50 of those outcomes are shown in Figure 9. The yield is increased from 18.4% to 66%, as shown in Figure 10. Once again, an excellent agreement is observed between the fine model response and the SM-based neuromodel response at the optimal yield solution $\mathbf{x}_{\text{SMBN}}^{Y*}$ (see Figure 11).

B. Considering Asymmetric Variations due to Tolerances

It is clear that our SM-based neuromodel assumes that the random variations in the physical design parameters due to the tolerances are symmetric (see Figures 1 and 3). To make a more realistic statistical analysis of the HTS filter, we consider that all the lengths and separations in the structure are asymmetric, as illustrated in Figure 12.

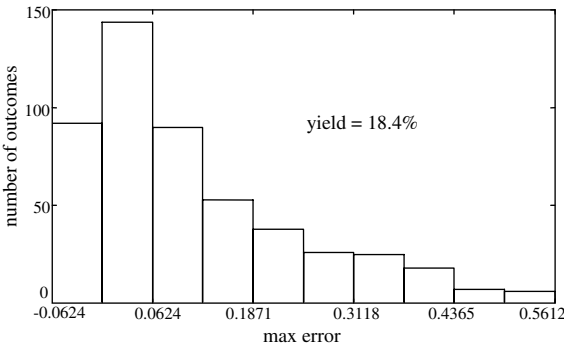


Figure 8. Histogram of the yield analysis of the SM-based neuromodel around the optimal nominal solution $\mathbf{x}_{\text{SMBN}}^*$ with 500 outcomes.

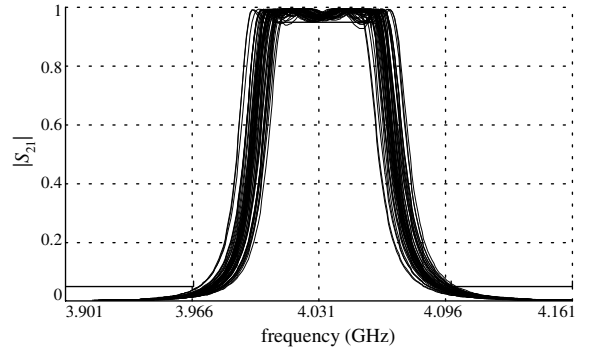


Figure 9. Monte Carlo yield analysis of the SM-based neuromodel responses around the optimal yield solution $\mathbf{x}_{\text{SMBN}}^{Y*}$ with 50 outcomes.

Developing a new SM-based neuromodel for this asymmetric structure would be very time consuming, because the dimensionality of the problem becomes very large, and many additional fine model training points would be needed. We have carried out several experiments that lead us to believe that the neuromapping obtained from symmetrical training data can be reused to build a first-order approximation of the fine model with asymmetric design parameter values. We propose the strategy illustrated in Figure 13. In this approach, we reuse the available neuromapping to take into account asymmetric random variations in the physical parameters due to their tolerances, taking advantage of the original asymmetric nature of the coarse model (compare Figures 3 and 13).

L_{1ac} and S_{1ac} in Figure 13 now represent the corresponding length and separation for the coarse model component in the left side of the structure (leftmost coupled-line module, see Figure 2), while L_{1bc} and S_{1bc} represent the corresponding dimensions for the right section

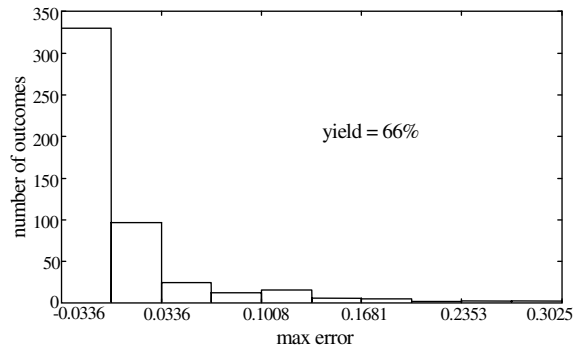


Figure 10. Histogram of the yield analysis of the SM-based neuromodel around the optimal yield solution $\mathbf{x}_{\text{SMBN}}^{Y*}$ with 500 outcomes (considering symmetry).

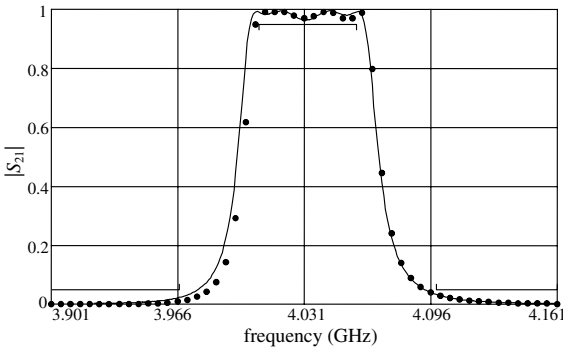


Figure 11. Fine model response and SM-based neuromodel response at the optimal yield solution $\mathbf{x}_{\text{SMBN}}^{y^*}$.

(rightmost coupled-line module, see Figure 2). Notice also that assigning a separate neuromapping to each of these sections (see Figure 13) makes physical sense, because the electromagnetic interaction between the microstrip lines in either the lower-left or upper-right parts of the structure is much larger than that one between the left-right or lower-upper microstrip lines.

Reusing the available neuromapping as described here avoids the need for extra fine model evaluations. A complete physical and mathematical justification is required. It will be addressed in future research. If generally valid, then taking into account the excellent generalization performance of our SM-based neuromodel, this approach should provide a good approximation to the yield considering that the tolerances are small.

We perform Monte Carlo yield analysis of the asymmetric SM-based neuromodel around the optimal nominal solution $\mathbf{x}_{\text{SMBN}}^*$ with 500 outcomes. The corresponding responses for 50 of

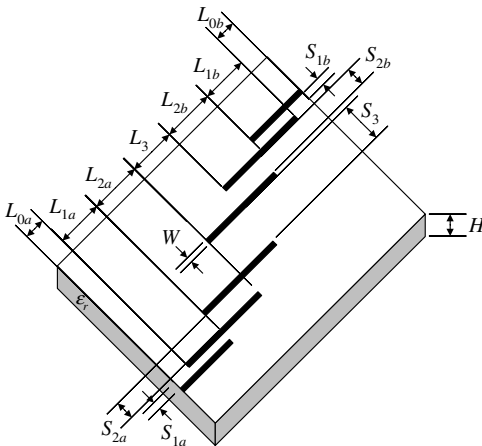


Figure 12. Physical structure of the HTS filter considering asymmetry.

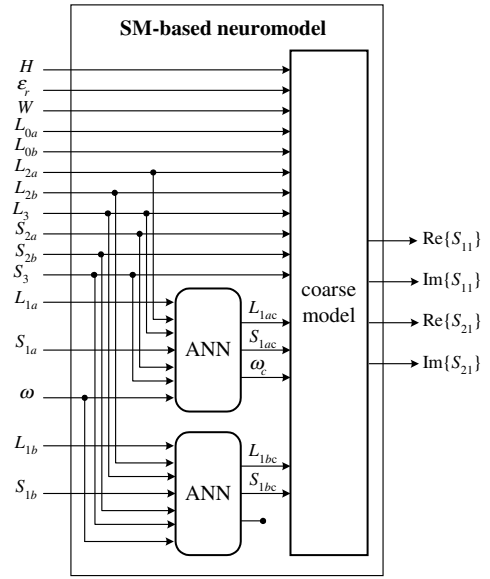


Figure 13. SM-based neuromodel of the HTS filter with asymmetric tolerances in the physical parameters (L_{1ac} and S_{1ac} represent the corresponding length and separation for the coarse model components in the left side of the structure—see Figures 1 and 2—while L_{1bc} and S_{1bc} represent the corresponding dimensions for the right section).

those outcomes are shown in Figure 14. The histogram of the yield at the optimal nominal solution $\mathbf{x}_{\text{SMBN}}^*$ with 500 outcomes is illustrated in Figure 15. A yield of only 14% was obtained for the asymmetric structure. We then perform Monte Carlo yield analysis of the asymmetric SM-based neuromodel around the optimal yield solution $\mathbf{x}_{\text{SMBN}}^{y^*}$ with 500 outcomes; 50 of those outcomes are illustrated in Figure 16. The yield obtained for the asymmetric structure is 68.8%, as illustrated in Figure 17.

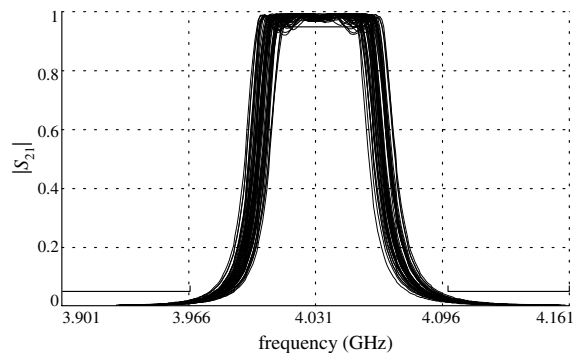


Figure 14. Monte Carlo yield analysis of the SM-based neuromodel responses, considering asymmetry, around the optimal nominal solution $\mathbf{x}_{\text{SMBN}}^*$ with 500 outcomes.

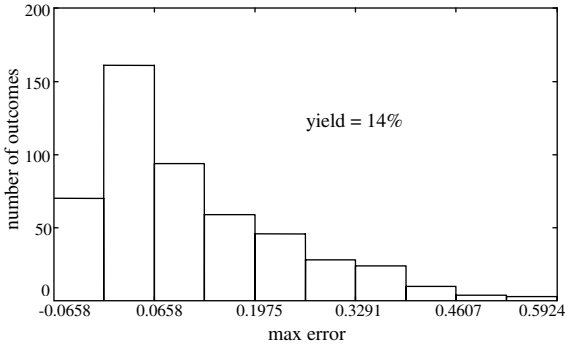


Figure 15. Histogram of the yield analysis of the asymmetric SM-based neuromodel around the optimal nominal solution $\mathbf{x}_{\text{SMBN}}^*$ with 500 outcomes.

VI. CONCLUSIONS

An efficient procedure to realize electromagnetics-based statistical analysis and yield optimization of microwave structures using space mapping-based neuromodels is proposed. We briefly review the use of neural networks for the design by optimization of microwave circuits. We mathematically formulate the problem of yield optimization using SM-based neuromodels. A general formulation for the relationship between the fine and coarse model sensitivities through a nonlinear, frequency-sensitive neuromapping is found. We avoid the need for extra EM simulations when asymmetric variations in the physical parameters due to tolerances are considered, by re-using the available neuromappings on asymmetric coarse models. We illustrate our techniques by the yield analysis and optimization of an HTS quarter-wave parallel coupled-line microstrip filter. The yield is increased from 14% to 69% for this complex structure. Excellent agreement between the

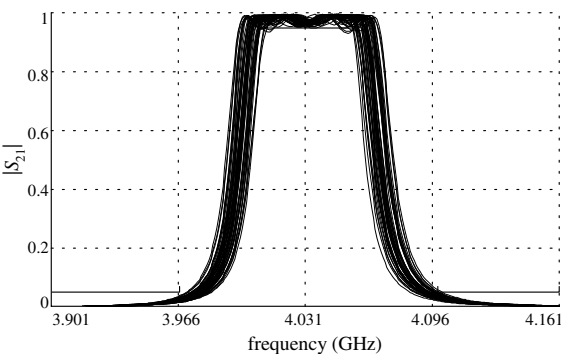


Figure 16. Monte Carlo yield analysis of the SM-based neuromodel responses, considering asymmetry, around the optimal yield solution $\mathbf{x}_{\text{SMBN}}^{Y*}$ with 50 outcomes.

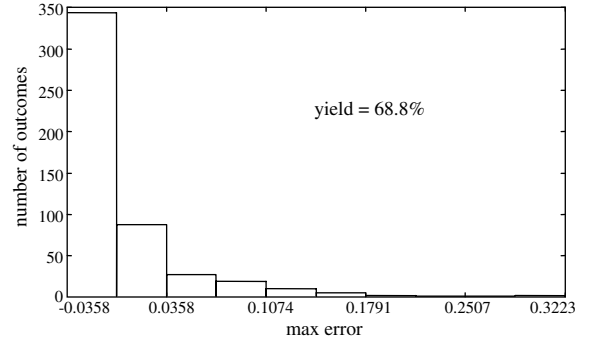


Figure 17. Histogram of the yield analysis of the asymmetric SM-based neuromodel around the optimal yield solution $\mathbf{x}_{\text{SMBN}}^{Y*}$ with 500 outcomes.

EM responses and the SM-based neuromodel responses is found at both the optimal nominal solution and the optimal yield solution.

ACKNOWLEDGMENT

The authors thank Dr. J.C. Rautio, President, Sonnet Software, Inc., Liverpool, NY, for making *em*TM available.

REFERENCES

1. J.W. Bandler, R.M. Biernacki, S.H. Chen, P.A. Grobelny, and S. Ye, Yield-driven electromagnetic optimization via multilevel multidimensional models, *IEEE Trans Microwave Theory Tech* 41 (1993), 2269–2278.
2. J.W. Bandler, R.M. Biernacki, S.H. Chen, and P.A. Grobelny, A CAD environment for performance and yield driven circuit design employing electromagnetic field simulators, *Proc IEEE Int Symp Circuits Syst Vol. 1*, London, England, 1994, pp. 145–148.
3. P. Burrascano and M. Mongiardo, A review of artificial neural networks applications in microwave CAD, *Int. J. RF and Microwave CAE*, Special Issue on Applications of ANN to RF and Microwave Design 9 (1999), 158–174.
4. J.W. Bandler, M.A. Ismail, J.E. Rayas-Sánchez, and Q.J. Zhang, Neuromodeling of microwave circuits exploiting space mapping technology, *IEEE Trans Microwave Theory Tech* 47 (1999), 2417–2427.
5. V.K. Devabhaktuni, M.C.E. Yagoub, Y. Fang, J. Xu, and Q.J. Zhang, Neural networks for microwave modeling: model development issues and nonlinear modeling techniques, *Int J RF and Microwave CAE* 11 (2001), 4–21.
6. T.S. Horng, C.C. Wang, and N.G. Alexopoulos, Microstrip circuit design using neural networks, *IEEE MTT-S Int Microwave Symp Digest*, Atlanta, GA, 1993, pp. 413–416.

7. A.H. Zaabab, Q.J. Zhang, and M.S. Nakhla, A neural network modeling approach to circuit optimization and statistical design, *IEEE Trans Microwave Theory Tech* 43 (1995), 1349–1358.
8. A. Veluswami, M.S. Nakhla, and Q.J. Zhang, The application of neural networks to EM-based simulation and optimization of interconnects in high-speed VLSI circuits, *IEEE Trans Microwave Theory Tech* 45 (1997), 712–723.
9. P.M. Watson and K.C. Gupta, Design and optimization of CPW circuits using EM-ANN models for CPW components, *IEEE Trans Microwave Theory Tech* 45 (1997), 2515–2523.
10. P. Burrascano, M. Dionigi, C. Fancelli and M. Mongiardo, A neural network model for CAD and optimization of microwave filters, *IEEE MTT-S Int Microwave Symp Digest*, Baltimore, MD, 1998, pp. 13–16.
11. P. M. Watson and K.C. Gupta, EM-ANN models for microstrip vias and interconnects in multilayer circuits, *IEEE Trans Microwave Theory Tech* 44 (1996), 2495–2503.
12. P.M. Watson, G.L. Creech, and K.C. Gupta, Knowledge based EM-ANN models for the design of wide bandwidth CPW patch/slot antennas, *IEEE AP-S Int Symp Digest*, Orlando, FL, 1999, pp. 2588–2591.
13. C. Cho and K.C. Gupta, EM-ANN modeling of overlapping open-ends in multilayer lines for design of bandpass filters, *IEEE AP-S Int Symp Digest*, Orlando, FL, 1999, pp. 2592–2595.
14. M.H. Bakr, J.W. Bandler, M.A. Ismail, J.E. Rayas-Sánchez, and Q.J. Zhang, Neural space mapping optimization of EM microwave structures, *IEEE MTT-S Int Microwave Symp Digest*, Boston, MA, 2000, pp. 879–882.
15. M.H. Bakr, J.W. Bandler, M.A. Ismail, J.E. Rayas-Sánchez, and Q.J. Zhang, Neural space mapping optimization for EM-based design, *IEEE Trans Microwave Theory Tech* 48 (2000), 2307–2315.
16. P.M. Watson, C. Cho, and K.C. Gupta, Electromagnetic-artificial neural network model for synthesis of physical dimensions for multilayer asymmetric coupled transmission structures, *Int J RF and Microwave CAE* 9 (1999), pp. 175–186.
17. J. Carroll and K. Chang, Statistical computer-aided design for microwave circuits, *IEEE Trans Microwave Theory Tech* 17 (1996), pp. 24–32.
18. Q.J. Zhang and K.C. Gupta, *Neural Networks for RF and Microwave Design*. Artech House, Norwood, MA, 2000.
19. J.W. Bandler and S.H. Chen, Circuit optimization: the state of the art, *IEEE Trans Microwave Theory Tech* 36 (1988), pp. 424–443.
20. OSA90/hope™ and Empipe™, ver. 4.0, formerly Optimization Systems Associates Inc., P.O. Box 8083, Dundas, ON, Canada, L9H 5E7, now Agilent Technologies, 1400 Fountaingrove Parkway, Santa Rosa, CA 95403-1799, 1997.
21. M.H. Bakr, J.W. Bandler, N. Georgieva, and K. Madsen, A hybrid aggressive space-mapping algorithm for EM optimization, *IEEE Trans Microwave Theory Tech* 47 (1999), pp. 2440–2449.
22. *em*™ ver. 4.0b, Sonnet Software, Inc., 1020 Seventh North Street, Suite 210, Liverpool, NY 13088, 1997.
23. R.R. Mansour, An engineering perspective of microwave CAD design tools, workshop notes on Automated Circuit Optimization Using Electromagnetic Simulators, *IEEE MTT-S Int Microwave Symp Digest*, Boston, MA, 2000.

BIOGRAPHIES



John W. Bandler was born in Jerusalem, on November 9, 1941. He studied at Imperial College of Science and Technology, London, England, from 1960 to 1966. He received the B.Sc.(Eng.), Ph.D. and D.Sc.(Eng.) degrees from the University of London, London, England, in 1963, 1967 and 1976, respectively.

He joined Mullard Research Laboratories, Redhill, Surrey, England in 1966. From 1967 to 1969 he was a Postdoctorate Fellow and Sessional Lecturer at the University of Manitoba, Winnipeg, Canada. Dr. Bandler joined McMaster University, Hamilton, Canada, in 1969. He has served as Chairman of the Department of Electrical Engineering and Dean of the Faculty of Engineering. He is currently Professor Emeritus in Electrical and Computer Engineering, directing research in the Simulation Optimization Systems Research Laboratory. He is a member of the Micronet Network of Centres of Excellence.

Dr. Bandler was President of Optimization Systems Associates Inc. (OSA), which he founded in 1983, until November 20, 1997, the date of acquisition of OSA by Hewlett-Packard Company (HP). OSA implemented a first-generation yield-driven microwave CAD capability for Raytheon in 1985, followed by further innovations in linear and nonlinear microwave CAD technology for the Raytheon/Texas Instruments Joint Venture MIMIC Program. OSA introduced the CAE systems RoMPE™ in 1988, HarPE™ in 1989, OSA90™ and OSA90/hope™ in 1991, Empipe™ in 1992, Empipe3D™ and EmpipeExpress™ in 1996. OSA created the product *empath*™ in 1996 which was marketed by Sonnet Software, Inc., USA. Dr. Bandler is President of Bandler Corporation, which he founded in 1997.

Dr. Bandler was an Associate Editor of the *IEEE Transactions on Microwave Theory and Techniques* (1969–1974), and has continued serving as a member of the Editorial Board. He was Guest Editor of the Special Issue of the *IEEE Transactions on Microwave Theory and Techniques* on Computer-Oriented Microwave Practices (1974) and Guest

Co-Editor of the Special Issue of the IEEE Transactions on Microwave Theory and Techniques on Process-Oriented Microwave CAD and Modeling (1992). He joined the Editorial Boards of the International Journal of Numerical Modelling in 1987, the International Journal of Microwave and Millimeterwave Computer-Aided Engineering in 1989, and Optimization and Engineering in 1998. He was Guest Editor, International Journal of Microwave and Millimeter-Wave Computer-Aided Engineering, Special Issue on Optimization-Oriented Microwave CAD (1997), and Guest Editor, IEEE Transactions on Microwave Theory and Techniques, Special Issue on Automated Circuit Design Using Electromagnetic Simulators (1997). He is currently Co-Chair of the MTT-1 Technical Committee on Computer-Aided Design.

Dr. Bandler has published more than 335 papers from 1965 to 2001. He contributed to *Modern Filter Theory and Design*, Wiley-Interscience, 1973 and to *Analog Methods for Computer-aided Analysis and Diagnosis*, Marcel Dekker, Inc., 1988. Four of his papers have been reprinted in *Computer-Aided Filter Design*, IEEE Press, 1973, one in each of *Microwave Integrated Circuits*, Artech House, 1975, *Low-Noise Microwave Transistors and Amplifiers*, IEEE Press, 1981, *Microwave Integrated Circuits*, 2nd ed., Artech House, 1985, *Statistical Design of Integrated Circuits*, IEEE Press, 1987 and *Analog Fault Diagnosis*, IEEE Press, 1987.

Dr. Bandler is a Fellow of the Royal Society of Canada, a Fellow of the Institute of Electrical and Electronics Engineers, a Fellow of the Institution of Electrical Engineers (Great Britain), a Fellow of the Engineering Institute of Canada, a Member of the Association of Professional Engineers of the Province of Ontario (Canada) and a Member of the MIT Electromagnetics Academy. He received the Automatic Radio Frequency Techniques Group (ARFTG) Automated Measurements Career Award in 1994.



José Ernesto Rayas-Sánchez was born in Guadalajara, Jalisco, Mexico, on December 27, 1961. He received the B.Sc. degree in Electronics Engineering from the Instituto Tecnológico y de Estudios Superiores de Occidente (ITESO), Guadalajara, Mexico, in 1984, and the Master's degree in Electrical Engineering from the Instituto Tecnológico y de Estudios Superiores de Monterrey (ITESM), Monterrey, Mexico, in 1989. He obtained the Ph.D. degree in Electrical Engineering from McMaster University, Hamilton, Ontario, Canada, in 2001.

He became a faculty member in the Electrical and Computer Engineering Department, ITESO, in 1989. He was on leave from his position from 1997 to 2001 to pursue doctoral studies in the Simulation Optimization Systems Research Laboratory, McMaster University. He returned to ITESO in 2001. His current research focuses on the development of novel methods and techniques for computer-aided modeling, design and optimization of analog wireless electronic circuits and devices exploiting Space Mapping (SM) and Artificial Neural Networks (ANN).

Dr. Rayas-Sánchez was the recipient of a 1997–2000 Consejo Nacional de Ciencia y Tecnología (CONACYT) scholarship awarded by the Mexican Government, as well as a 2000–2001 Ontario Graduate Scholarship (OGS) awarded by the Ministry of Training for Colleges and Universities in Ontario.



Qi-jun Zhang received the B.Eng. degree from East China Engineering Institute, Nanjing, China in 1982, and the Ph.D. degree in Electrical Engineering from McMaster University, Hamilton, Canada, in 1987.

He was with the System Engineering Institute, Tianjin University, Tianjin, China in 1982 and 1983. During 1988–1990, he was with Optimization Systems Associates Inc. (OSA), Dundas, Ontario, Canada, developing advanced microwave optimization software. He joined the Department of Electronics, Carleton University, Ottawa, Canada in 1990, where he is presently a Professor. His research interests are neural network and optimization methods for high-speed/high-frequency circuit design, and has over 150 articles in the area. He is a co-author of *Neural Networks for RF and Microwave Design* (Artech House, Boston, 2000), a co-editor of *Modeling and Simulation of High-Speed VLSI Interconnects* (Kluwer, Boston, 1994), a contributor to *Analog Methods for Computer-Aided Analysis and Diagnosis*, (Marcel Dekker, New York, 1988), a Guest co-Editor for a Special Issue on High-Speed VLSI Interconnects for the *International Journal of Analog Integrated Circuits and Signal Processing* (Kluwer, Boston, 1994), and Guest Editor for the Special Issues on Applications of ANN to RF and Microwave Design for the *International Journal of RF and Microwave CAE* (Wiley, New York, 1999).

Dr. Zhang is a senior member of the IEEE and member of the Professional Engineers Ontario.